Infrared Physics and Technology 104 (2020) 103141

Contents lists available at ScienceDirect

Infrared Physics & Technology

journal homepage: www.elsevier.com/locate/infrared

Regular article

Laser line scanning thermography for surface breaking crack detection : modeling and experimental study

Nithin Puthiyaveettil[a,*], K Renil Thomas[a], Sreedhar Unnikrishnakurup[a], Philipp Myrach[b], Mathias Ziegler[b], Krishnan Balasubramaniam[a]

[a] Indian Institute of Technology Madras, Chennai, India
[b] Federal Institute for Materials Research and Testing (BAM), 12200 Berlin, Germany

ARTICLE INFO

Keywords:
Infrared thermography
Laser line scanning
Surface breaking cracks
FEM

ABSTRACT

Crack detection in metallic samples at high surface temperature, hostile and hazardous environments, etc. is a challenging situation in any manufacturing industries. Most of the present NDE methods are suitable only for lower surface temperatures, especially at room temperature. In this situation, we need a fast and non-contact NDT method which can be applied even in high sample surface temperature. Laser thermography is one of the techniques having a high potential in non-contact inspection. As a preliminary investigation, in this article, we have studied the potentiality of laser line thermography in crack detection at room temperature. In laser line thermography, a continuous wave (CW) laser is used to generate a laser line, which in turn is used to scan the metal surface. The heat distribution over the sample surface is recorded by an infrared thermal (IR) camera. Two different approaches are reported in this work. Firstly, a stationary laser line source and its interaction with cracks; secondly, moving laser line source scanning over a surface with crack. When the distance between crack centre to laser line centre increases, crack detectability will decrease; and when laser power increases, crack detectability will increase. A dedicated image processing algorithm was developed to improve the detectability of the cracks. To understand the heat transfer phenomenon, a simplified 3D model for laser thermography was developed for the heat distribution during laser heating and was validated with experimental results. Defects were incorporated as a thermally thin resistive layer (TTRL) in numerical modeling, and the effect of TTRL in heat conduction is compared with experimental results.

1. Introduction

Surface breaking cracks are one of the critical issues in steel manufacturing industries. The life of any component depends on the presence of cracks in it. Presently many NDT methods are available for crack detection at room temperature, like ultrasound testing, liquid penetrant testing, magnetic particle inspection, computer tomography, eddy current testing, etc. Selection of an NDT method for the detection of cracks depends on the size and complexity of the sample, sample temperature and working environments [1]. Presently minimal NDT methods are available that have the capability of crack detection in a hostile and hazardous environment, where direct accessibility of sample is not possible. Infrared (IR) thermography is one of the promising NDT methods known for its fast and non-contact way of defect detection. In conventional active thermography, the sample surface is homogeneously heated by using flash lamps or any other external heat source [2]. An IR camera is used to capture the heat distribution over the surface. When the sample surface is spatially homogenously heated, the heat flow inside the sample will be restricted only in the in-depth direction. Presence of defects in the direction of heat flow will alter the thermal distribution and can be identified in the thermogram [3]. The surface breaking cracks oriented perpendicular to the surface are very critical and not affected much by the heat flow. Hence, it is challenging to detect the cracks which are oriented perpendicular to the surface when using flash thermography. To tackle this problem, research during the last few years has identified laser-thermography (LT) as a powerful thermographic technique to identify surface breaking cracks [4–6]. In LT, a focused laser beam is used to heat the sample surface locally, and an IR camera is used to capture the variation in thermal distribution over the surface due to the presence of cracks. Since both the IR camera and the laser are operating at a distance from the object, LT is purely non-contact in operation; it can handle the hostile

* Corresponding author at: Centre of Non-Destructive Evaluation (CNDE), Machine Design Section, Dept. of Mechanical Engineering, Indian Institute of Technology Madras, Room No: 312, Chennai 600036, India.
E-mail address: nithinvengara@gmail.com (N. Puthiyaveettil).

https://doi.org/10.1016/j.infrared.2019.103141
Received 20 August 2019; Received in revised form 30 October 2019; Accepted 22 November 2019
Available online 29 November 2019
1350-4495/

environment and can be employed for measurement of defect detection and measurement of process and product parameters.

The concept of flying spot thermography was introduced in the late 1960s by Kubiak et al. [7]. The technique was developed over the next few decades; following the advancements in infrared (IR) detector, laser technology became a promising tool [8]. Selection of laser type, i.e. Pulsed laser or continues wave (CW), and shape of the laser beam (spot, line or area) depend on the application, sample material, etc. [2]. In laser spot thermography, a laser beam is used to produce a laser spot, which is in turn used to heat the sample surface. Any disturbance present in the direction of heat flow will alter the thermal heat distribution and can be recorded using an IR camera [5,9–11]. The scanning rate can be increased by using a laser line to scan the sample surface instead of a laser spot. Hence, fast detection of cracks is possible. Some preliminary experimental studies have shown the capability of laser line scanning in detecting surface breaking cracks [12–16]. Li et al, established and developed a fast crack detection algorithm using a laser line scanning thermography in room temperature. 3D finite difference modelling (FDM) results are presented that show the sensitivity of the laser line thermography technique to cracks of varying lengths, depths and openings [12]. Hwang et al presents a continuous-wave line laser thermography system for monitoring of rotating wind turbine blades. This paper shows the application of laser line thermography in Inservice inspection using a dedicated image processing algorithm. But this paper not explaining any numerical simulations [13]. Numerical simulation studies are important for better understanding of the phenomenon behind laser thermography. Some research groups have proposed numerical models of both laser spot scanning and laser line scanning thermography for further detailed parameter studies [17–22].

The main objective of this paper is to develop a validated Finite Element Model (FEM) for better understanding of physics and can be utilised for the further studies. In comparison with FDM, FEM will permit to get a higher order of accuracy, but requires more computational power and is also more exigent on the quality of the mesh. FEM permits multi-physics analysis, and complex geometry domain cases much easier. Presence of a defect is approximated using a surface boundary condition (Thin thermally resistive layer) in modelling. A simple defect tracking algorithm developed for real time crack detection. Mainly two types of laser heating mechanisms namely stationary laser line source and moving laser line source were studied. The stationary laser line is used to heat the sample for a finite period of time. The presence of a surface breaking defect will alter the thermal distribution and can be recorded using an IR camera. The effect of distance between the laser line centre and defect centre in crack detection is studied here. The second case is laser line scanning, where there is a relative motion between the laser line and the sample. A laser line is used to scan the sample surface. The effect of laser power in crack detection is studied here. 3D numerical models are developed for both laser line stationary study and laser line scanning study for understanding the physics. Simulation results are validated with the experimental results. Laser based experiments are expensive and risky, developing a validated FEM model can be used for process parameter optimisation.

The paper is organized as follows: following a brief description of the experimental setup and experimental procedure, a simplified 3D heat diffusion phenomenon is modelled for laser line thermography. The simulation results are validated with experimental cases. Defects are incorporated as a thin thermally resistive layer (TTRL) in numerical modeling, and the effect of TTRL in heat conduction is compared with an experimental defect. A dedicated data processing algorithm is developed for better detection of defects. The paper concludes with directions for future work.

2. Theory

The presence of cracks or discontinuity in the sample will disturb the heat distribution in the sample. This variation in temperature profile can be visualised using an IR camera. Fig. 1 is the schematic diagram of laser thermography. A focused laser beam is used to heat the metal surface locally. In the case of flash thermography, the entire area is assumed to be uniformly heated. Hence, heat diffusion will be one-directional (in-depth direction). But in the case of local heating, the heat flow is not only in the in-depth direction but also in the planar direction.

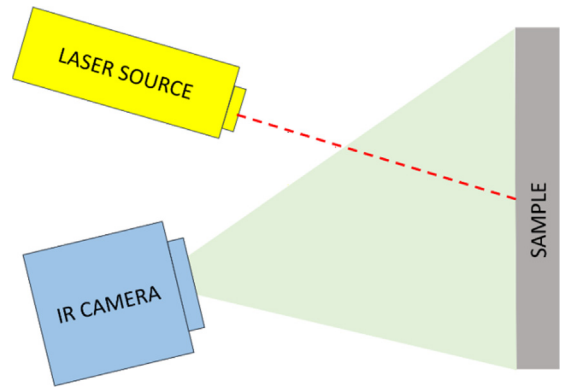

Fig. 1. Schematic diagram of laser thermography: A focused laser beam is used to heat the metal surface locally and heat distribution is viswalized using an IR camera.

Fig. 2 is the schematic diagram of different instances of laser interaction with sample such as without any defect, laser beam near to the defect and falling inside the crack. (a) Shows the heat distribution profile with the laser beam incident on a non-defective area; 3D heat diffusion will happen into the bulk material. (b) Here crack edges will act as barrier for heat flow and lead to rise in temperature than the first case. And in the third case (c), the laser source might fall directly into the crack opening. The latter two cases are the two major mechanisms by which a surface breaking crack leads to an increase in temperature. The first mechanism is heat-blockage due to the presence of a crack, predominantly oriented perpendicular to the surface will alter the heat diffusion profile and lead to a considerable temperature contrast on the surface. Capturing and analysing the surface temperature on the sample surface using an IR-camera leads to crack detection.

The second mechanism is optical entrapment (Fig. 2(c)). In this case, when a laser beam interacts with a crack, multiple reflections in the crack inner surfaces increase the effective absorption and such a more efficient heating results in higher crack temperature. The crack will act similar to a black body wherein majority of energy will get absorbed. Thus heating is more efficient within the crack. Furthermore, due to the black body effect the crack acts as a good emitter of IR-radiation due to its increased surface area compared to the flat surface. Both effects lead to a higher temperature recorded by the IR-camera at the place of a crack.

3. Methodology

In order to demonstrate the capability of the laser line scanning

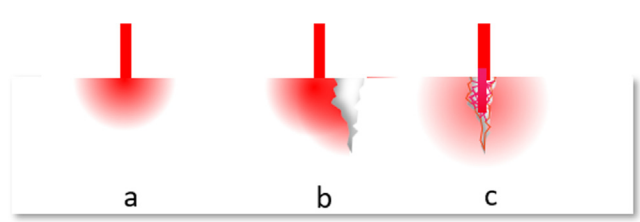

Fig. 2. Schematic diagram of laser beam heating (a) when there is no defect (b) Near to the crack edge (c) Inside a crack.

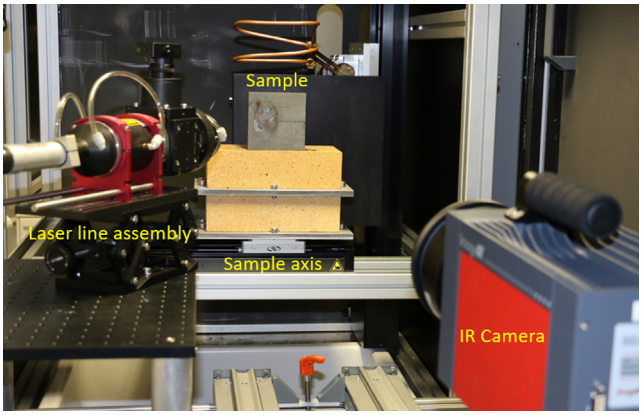

Fig. 3. Laser thermography experimental set up with essential components.

thermography in crack detection, we carried out some initial experiments. A numerical model developed for the laser scanning thermography and this validated model used for the further studies.

3.1. Experimental setup

Experiments were carried out in laser thermography equipment and the necessary safety concerns being taken in to account. Fig. 3 shows the laser thermography set up with essential components. A CW diode laser with a maximum output power of 510 W and a wavelength of 940 nm was used to produce a laser line with the help of beam shaping assembly (line length = 30 mm × 0.6 mm). The sample was placed on a translation stage with a maximum speed of 100 mm/s. A calibrated IR camera with a necessary calibration file was used to monitor the thermal profile over the sample.

In the present study, additional optics were used to create a line to achieve high testing speed. A photograph of the laser line assembly is shown in Fig. 4. All the experiments were performed with the sample at room temperature (RT). The sample under study was a block made of ST37 steel, 100 mm in length, 100 mm in width and 40 mm in depth, containing notches of different depths. Fig. 5(a) is the scheme of the specimen with the notch positions and the respective depths indicated. All notches are 30 mm in length and 0.2 mm in width. Fig. 5(b) shows the photograph of the specimen made of ST37 steel.

3.2. Numerical modeling

A numerical model for heat transfer phenomenon during laser line heating was developed using a commercial finite element(FE) package. The thermo-physical properties of the steel sample used in the

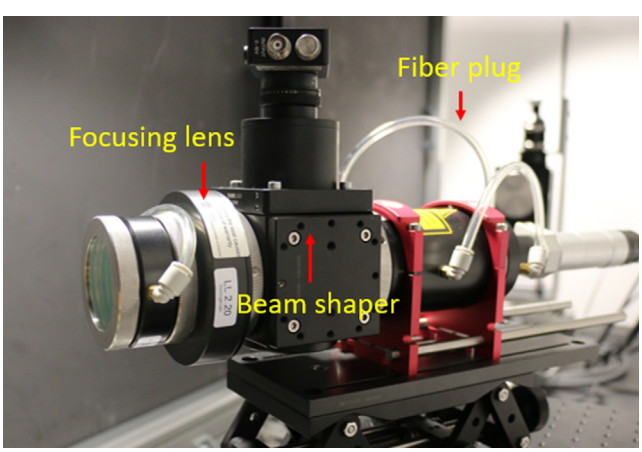

Fig. 4. Laser line assembly: convert the laser beam to laser line.

numerical simulation are given in Table 1. The model geometry was according to the sample and the heat source according to the laser used. A rectangular block of steel having 100 mm length, 100 mm width and 40 mm thickness. A notch having opening 0.2 mm, length 30 mm and depth 2.2 mm was introduced in the block. A laser line beam, 30 mm in length and 0.6 mm in width, was used to heat the sample; the initial temperature of the sample was set to room temperature.

Illuminating the metal sample surface generates a temperature gradient, due to which an energy transfer will occur from the high-temperature to the low-temperature region. The heat transfer rate due to conduction per unit area is proportional to the normal temperature gradient:

$$\frac{q}{A} = -k\frac{\partial T}{\partial n} \tag{1}$$

where q is the heat transfer rate, $\frac{\partial T}{\partial n}$ is the temperature gradient in the direction of the heat flow, and $k$is the thermal conductivity of the material ($W*m^{-1}*K^{-1}$). The negative sign indicates that heat flows from a higher to a lower temperature area. Considering the energy balance in three dimensions, The equation for transient 3D heat transfer in solids can be written in the following form:

$$\rho C_p\frac{\partial T}{\partial t} - \frac{\partial}{\partial x}\left(k_x\frac{\partial T}{\partial x}\right) - \frac{\partial}{\partial y}\left(y\frac{\partial T}{\partial y}\right) - \frac{\partial}{\partial z}\left(k_z\frac{\partial T}{\partial z}\right) = Q \tag{2}$$

Q is the heat source or sink, ρ is the density of the material, C_p is the specific heat of the material ($J*kg^{-1}*K^{-1}$), k_x, k_y, k_z are the thermal conductivities in the x, y and z direction respectively, T is temperature and t is the time.

The ambient temperature is taken as room temperature (T_0 = 300 K) for all domains. Table 1 gives the thermal properties of the ST37 steel.

Local heating of the metal surface using laser beam assumes that the beam energy is absorbed over a minimal distance into the material (absorption length) compared to the size of the object which is heated. Very refined triangular mesh elements are incorporated near to the laser line, maximum element size of 0.1 mm. The power density of the laser line is given in Eq. (3)

$$\varphi = A\cdot P\cdot f(Y)\cdot\frac{1}{\sigma_X\sqrt{2\pi}}e^{\frac{-(X-X_0-v\cdot t)^2}{2\sigma_X^2}} \tag{3}$$

where A is the absorption factor which depends on the laser wavelength (940 nm in this study), P is the laser power, f is rectangular function is used to generate a rectangular-shaped pulse for input to the FE model. In this study the width of the rectangular function is 0.6 mm and height is unity. σ_x represents the radius of the laser at 1/e of amplitude on X-direction, v is the scanning velocity(in static study, v = 0), and X_0 is the laser line beam origin point in X axis. The laser irradiance of the line beam is supposed to be a top hat profile but was measured .to be gaussian in X axis. A rect function was used in order to achive a rectangular iradiance in Y direction. A simulated laser line thermal profile during the laser excitation is shown in Fig. 6.

When a defect is introduced in the model, the heat transfer is altered. This phenomenon can be handled in the numerical model by introducing an obstruction for the heat flow. To achieve this, an interior boundary condition known as Thin Thermal Resistive Layer (TTRL) has been introduced as a defect. This boundary condition can be expressed as:

$$-n_l\cdot(-k_l\nabla T_l) = -\frac{T_u - T_l}{R_S} \tag{4}$$

$$-n_u\cdot(-k_u\nabla T_u) = -\frac{T_l - T_u}{R_S} \tag{5}$$

$$R_S = \frac{d_S}{k_S} \tag{6}$$

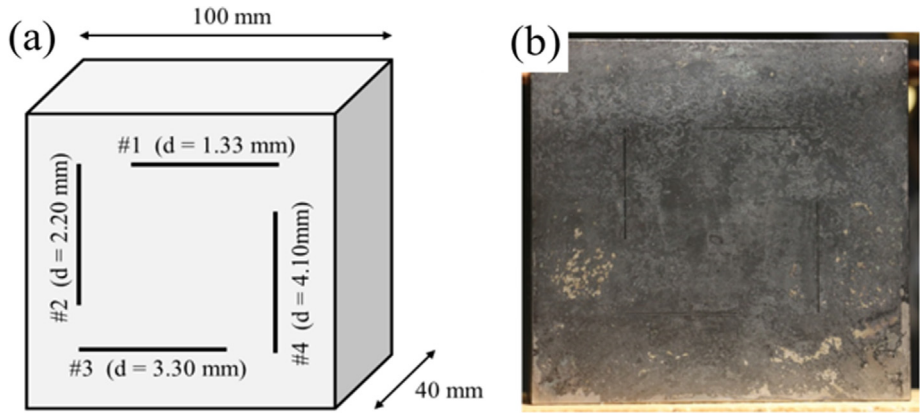

Fig. 5. Specimen made of ST37 steel (All notches are 30 mm in length and 0.2 mm in width).

Table 1
Temperature-dependent material properties of steel used in simulation.

Property at 20 °C	Thermal conductivity (W ∗ m − 1 ∗ K − 1)	Density (kg /m^3)	Specific heat (J ∗ kg − 1 ∗ K − 1)
	40.49	421.3	7821

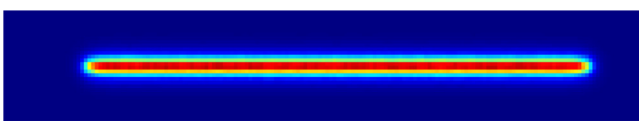

Fig. 6. Simulated laser line thermal profile at t = 10 ms.

where the subscripts u and l represent the upper and lower surfaces of the thin layer. R_s is the thermal resistance across the layer as in Eq. (6), $d_s$is the thickness of the layer, and k_s is the layer conductivity, the layer thickness used in the model is 0.2 mm and the thermal conductivity used is that of air.

Fig. 7(a) shows the meshed geometry and Fig. 7(b) shows the surface temperature evolution obtained from the model. In the second case, we introduced a rectangular notch with 0.2 mm width, 30 mm length and 2.2 mm depth, in the model. Although both the models handled the phenomenon and gave acceptable temperature profile, using TTRL, the computational time reduced noticeably (180 min). An extremely fine mesh was employed in the domain surface where the heat source was applied, and a relatively coarser mesh was employed in the remaining part of the domain. A time-dependent solver with a maximum time step of 0.001 s was employed for computation. A desktop with a CPU frequency of 3.31 GHz and memory of 16 GB was used to solve the models; it took 180 min for the simulation.

3.3. Experimental validation

We carried out several preliminary experiments to validate the model using a laser line beam to heat the sample. There was no relative motion between the laser line and the sample. A laser power of 50 W was used to produce the laser line and the sample was heated for 66 ms. An IR camera with a frame rate of 200 Hz was used to capture the thermal distribution over the sample. The same experiments were carried out for the sample without a defect and with a defect. The distance between the centre of the laser line and the notch centre was kept as 1 mm for the defective case. Fig. 8 shows the surface temperature distribution of both defective and non-defective cases. Fig. 8a shows the simulation results of the surface temperature distribution of the non-defective case, heat distribution over the sample surface is symmetric when there is no notch near to the laser line. When a defect was introduced near to the laser line, the heat distribution got altered and leading to an increased temperature contrast is shown in Fig. 8b. Fig. 8c shows the surface temperature distribution of the non-defective case from the experiment and Fig. 8d shows the surface temperature distribution of the defective case from the experiment. Both experimental and modeling results are showing the same trends in heat distribution, i.e. the numerical results are compromising with the experimental results.

A reference line probe was considered across the laser line beam and

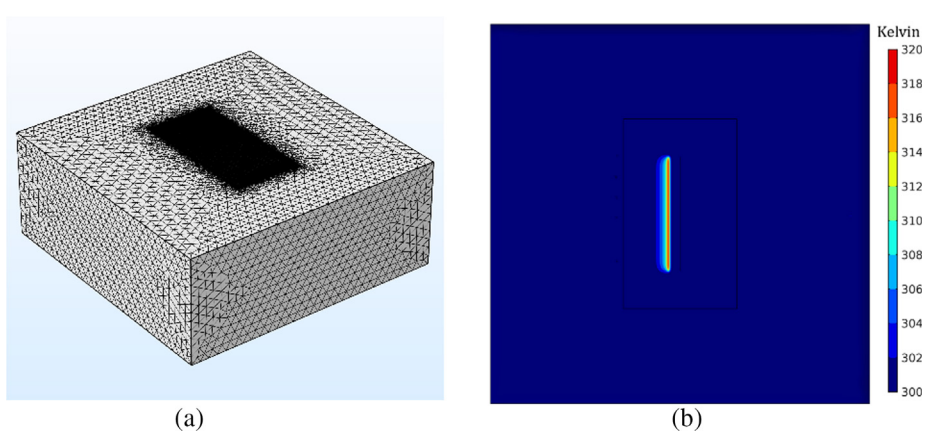

Fig. 7. FEM simulation (a) Meshed geometry (b) Surface temperature profile after simulation.

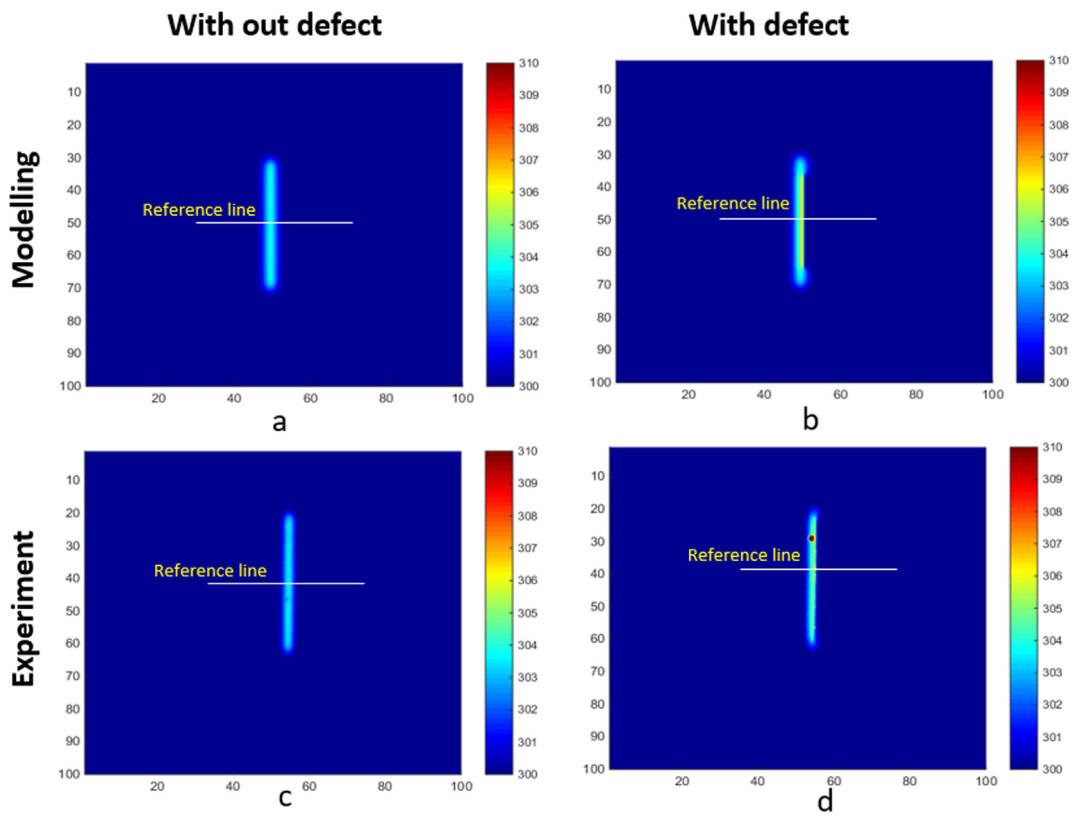

Fig. 8. Surface temperature distribution of defective and non-defective cases. (a) Simulation results non-defective case (b) Simulation results defective case (c) Experimental results non-defective case (d) Experimental results defective case.

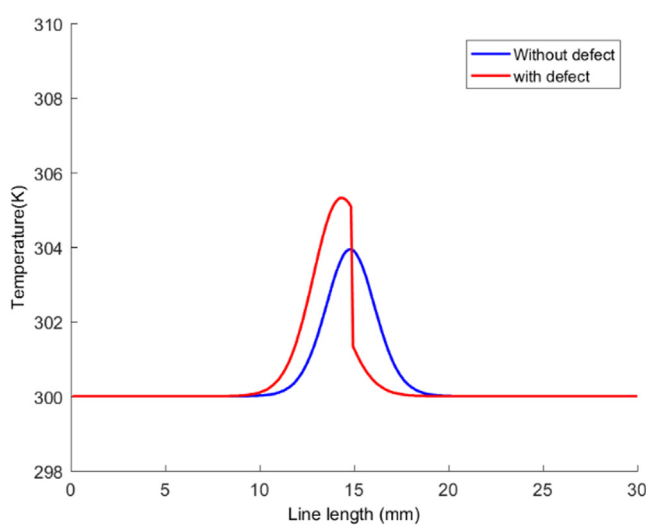

Fig. 9. Temperature plot of the reference line for modeling.

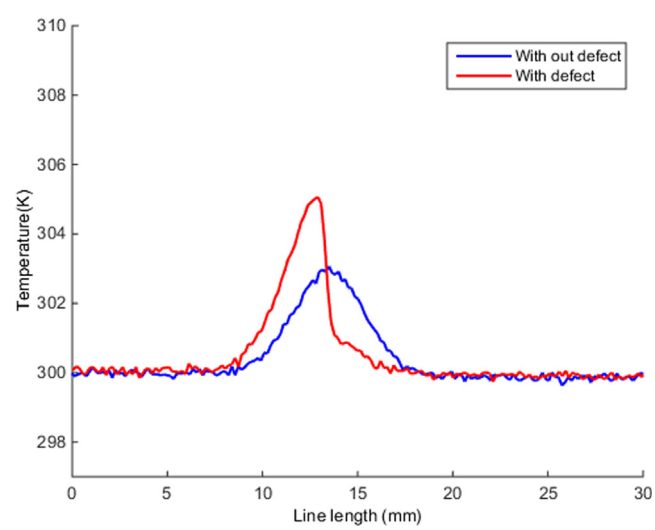

Fig. 10. Temperature plot of the reference line for experiment.

the temperature distribution over the probe has been plotted. The same procedure is followed for both defective and non-defective cases at the same instance of time. Fig. 9 shows the temperature plot of the reference line for modeling, wherein the blue line indicates the temperature distribution of the reference line when there is no defect. The heat distribution appears as uniform and symmetric to the centre of laser line because there is no disturbance in 3D heat diffusion. The presence of the notch blocks the heat diffusion which leads to heat accumulation and is indicated as a sudden peak in the reference line plot (red line). Fig. 10 shows the reference line plot for the experimental results. Here also, the red line indicates the reference line plot of the defective case and the blue line corresponds to the non-defective case. Heat diffusion is altered due to the presence of the notch. Fig. 10 shows the experimental results; here we can see the same trend as in modelling.

4. Results and discussion

Two types of studies are done in this paper

1) Laser line stationary study (There is no relative motion between laser line and sample)
2) Laser line scanning study (There is a relative motion between laser line and sample)

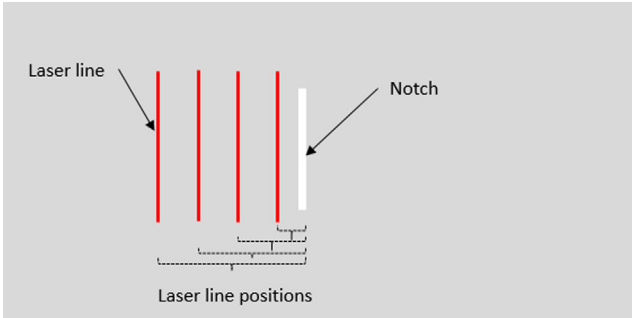

Fig. 11. Varying the distance between laser line centre and crack centre.

4.1. Laser line stationary study

In the laser line stationary case, there is no relative motion between the laser line and the sample. The distance between the notch centre and laser line centre is kept as 1 mm and the laser line switched on for 66 ms. The heat distribution over the sample surface is recorded using a thermal camera. The same procedure was repeated for four main cases by varying the distance between the laser line centre and notch centre, by 1 mm, 2 mm, 4 mm and 6 mm away. The surface heat distribution variation due to the presence of a defect was studied. Fig. 11 is the schematic representation of different laser positions with respect to the notch centre.

The presence of notch will cause anomalies in the temperature behaviour which is captured by the IR camera. Accordingly, the temperature history of pixels near the crack should be analysed in detail to extract the contrast image. A dedicated algorithm was developed using MATLAB for the analysis. The procedure of the algorithm is as follows in Fig. 12:

(1) Consider a line probe across the laser line in raw data. (2) Note the temperature profile of the line probe in each frames (3) Take the 1st derivative of these temperature plots of line profile. (4) Identify the frame number or time (t_{max}) where the defect signal is showing the maximum intensity in the 1st derivative plot. (4) Identify corresponding frame at t_{max} from the raw data (5) Take spatial derivative of the identified frame. These five steps are shown in the Fig. 12 The same procedure is applied for all the cases – 1 mm, 2 mm, 4 mm and 6 mm away.

Fig. 13 shows the temperature profiles of the line probe obtained from simulation. Thermal heat blockage due to the presence of a notch is visible for all cases. Here, the maximum temperature rise due to heat blockage is achieved when the distance between the laser line centre and notch centre is kept as 1 mm away, and is indicated by the red line. The black line, for 6 mm away, shows the lowest temperature rise due to the notch. When there is a defect, there will be a increased temperature due to the blockage is appears as a sudden variation in the temperature plot. The peak of the temperature plot decreases with an increase in the distance between the laser line centre and notch centre. Fig.14 shows the temperature profile of the line probe obtained from the experimental results and exhibits the same trend as that of the simulation. The temperature profile of the probe in both experimental data and modeling data gives a clear indication of a defect.

The detection of the notch depends on the rise in temperature due to heat blockage. Rise in temperature can be termed as thermal contrast (differnce between the peak temperature and the surface temperature), which is the measure of defect detectability. Fig. 15 shows the relation between thermal contrast and laser line position with respect to the notch centre. Here, the blue line shows the numerical simulation and the red line corresponds to experiments. From the graph, it is clear that

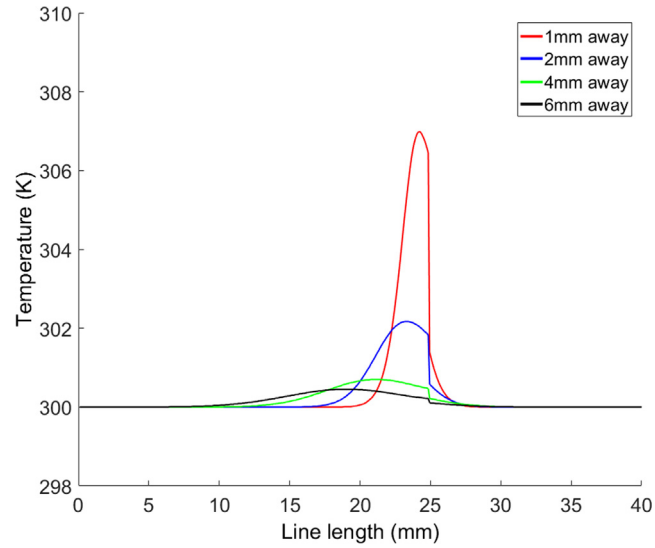

Fig. 13. Temperature profiles of the line probe for simulation.

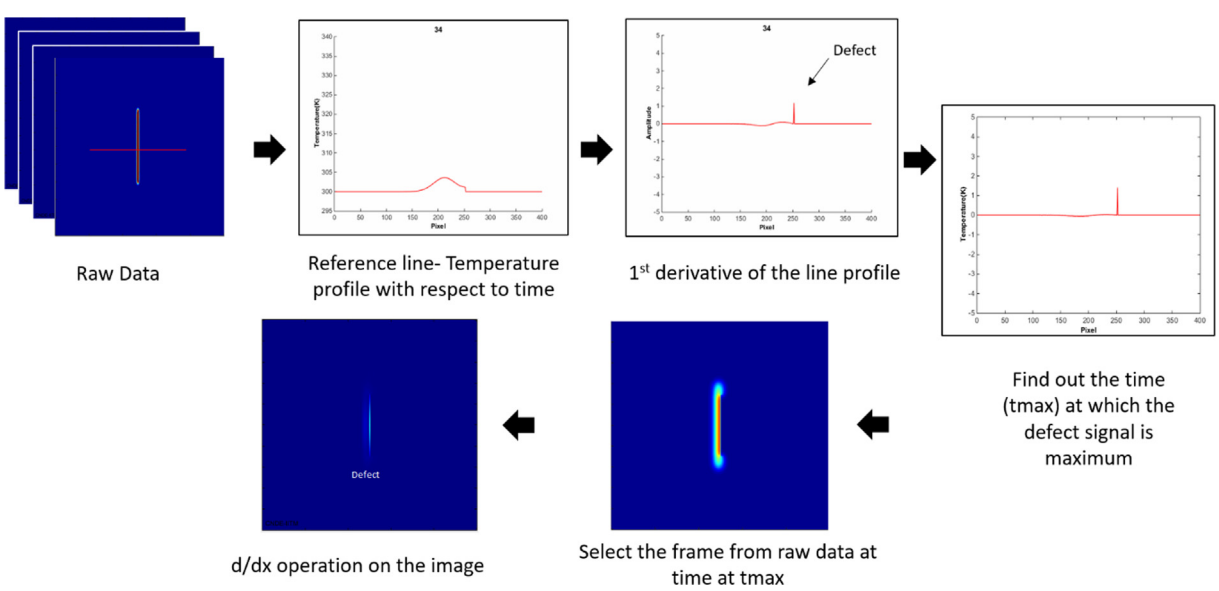

Fig. 12. Procedure for crack detection algorithm.

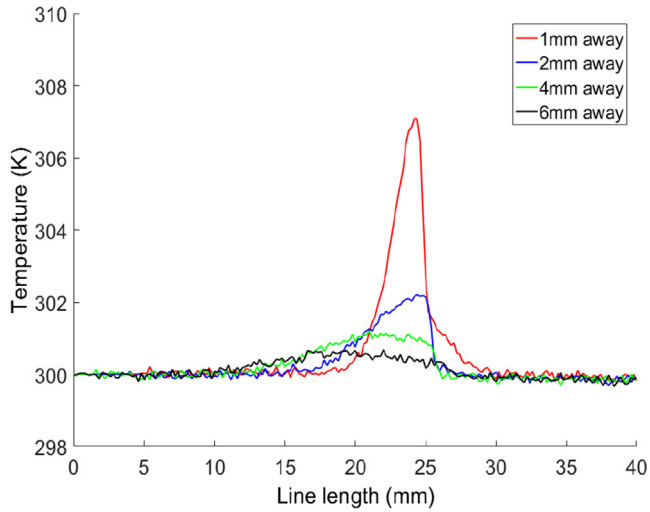

Fig. 14. Temperature profiles of the line probe for experiment.

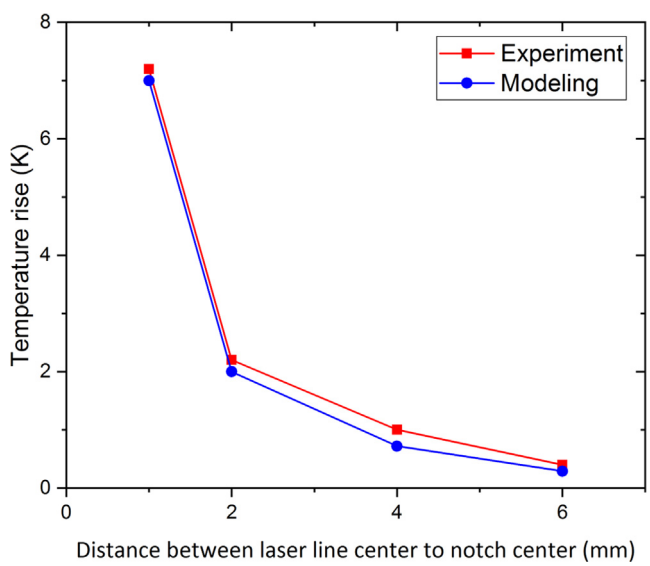

Fig. 15. Relation between the thermal contrast and laser line distance from notch centre.

when the distance between the laser line centre and notch centre increases, the intensity of heat blockage reduces, i.e. rise in temperature also reduces. In the case of 6 mm away and higher, the temperature rise becomes comparatively very small. Difference between the experiment and modelling result is mainly due to surface roughness of the sample and the emissivity issues.

Fig. 16 shows the processed images for experiments using the derivative algorithm; the processed images show a clear indication of defect. As discussed before, the notch contrast also decreases with increasing distance between the laser line centre and notch centre. In the processed images we can observe the work piece edges as two verticals lines.

4.2. Laser scanning study

In the case of laser scanning, the sample passes across the laser line at a constant velocity and gets heated. The 50 W laser energy was used to generate a 30 mm 0.6 mm line beam in size. The sample is moving at a constant velocity of 50 mm/s across the laser line. Unlike the laser line stationary case, in the laser scanning case, the laser beam was ON throughout the process. Hence, the algorithm developed for the laser line stationary case cannot be applied here. We developed another algorithm for the analysis of laser scanning study. In this algorithm, a small area A_1 (5 × 5 pixel) was following the laser line with the same speed (50 mm/s). The distance between the centre of A_1 to laser line centre was kept optimum and constant. The average temperature of the area A_1 was calculated in each frame and plotted with respect to time. Fig. 17 shows a frame from laser scanning.

The same procedures were carried out to check the effect of laser line power intensity in defect detectability for 50 W, 100 W, 150 W, 200 W and 250 W. The sample speed was kept constant at 50 mm/s in all the trail. Fig. 18 shows the average temperature of the area A_1 in all the frames of the modeling results. For better understanding, the graph is divided in to three zones ie, Zone A: where the notch is approaching to the monitoring area A_1, Zone B: where the notch is inside the monitoring area A_1 and Zone C: where the notch is moving away from the monitoring area A_1. In Zone A the average temperature of A_1 is gradually increasing with time due to the preheating but at the end of the zone A there is a sudden rise in average temperature due to the heat accumulation by the notch. The average temperature of the monitoring area is maximum when the notch reach exactly at the edge of the monitoring area. In zone B the notch is always present in the monitoring area A_1. The temperature rise at the both sides of the notch is different due to the heat blockage, so less heat is transfering from one side to the other. Thus preheating of the other side of the notch is hindered due to the presence of a notch. Hence in zone B, the average temperature of the monitoring area is decreasing with time due to the abscence of preheating. In Zone C, where the notch is moving away from to monitering area A_1, the effect of notch is reduced and average temperature of A_1 is gradually increasing with time due to the preheating as we discused in the initial part of zone A. When the laser power increases from 50 W to 250 W to produce the laser line, the average surface temperature rises from 308 K to 356 K. The temperature rise due to heat blockage is also increasing with an increase in laser power intensity. The notch was much more detectable when we used 250 W instead of 50 W to produce the laser line.

Fig. 19 shows the average temperature plot of the area A1 in the case of experimental results. The trends visible in the modeling results are also visible in experimental results. The results validate the model and allow further numerical studies.

Fig. 20 shows the relation between the temperature rise due to heat blockage and laser power. Difference between peak temperature due to the presence of notch and average surface temperature due to laser scanning is considered as the thermal contrast (rise in temperature). The graph reveals that temperature rise due to thermal blockage is increasing with increasing laser power used to produce the laser line. Both experiments and models give the same trends. Here, blue dots are the numerical simulation results and red dots stand for experimental results and all are closely matching with simulation trends.

5. Conclusion

The capability of laser line thermography in fast defect detection is established. A promising numerical model for laser line thermography was achieved using a commercial FE software package. Mainly two types of studies were reported in this paper namely, laser line stationary study and laser line scanning study. In the case of laser line stationary study, a laser line was used to heat the sample and there is no relative motion between the laser line and sample. The effect of distance between the laser line centre to defect centre in crack detection was studied here. When the distance between the laser line centre and notch centre increases, detectability decreases. In laser line scanning, there is a relative motion between the laser line and sample. The effect of laser line power intensity in crack detection was studied here. When the laser power increases, the notch detectability also increases. The models developed for both the cases were validated with the experimental results. Defects were incorporated as a thermally thin resistive layer

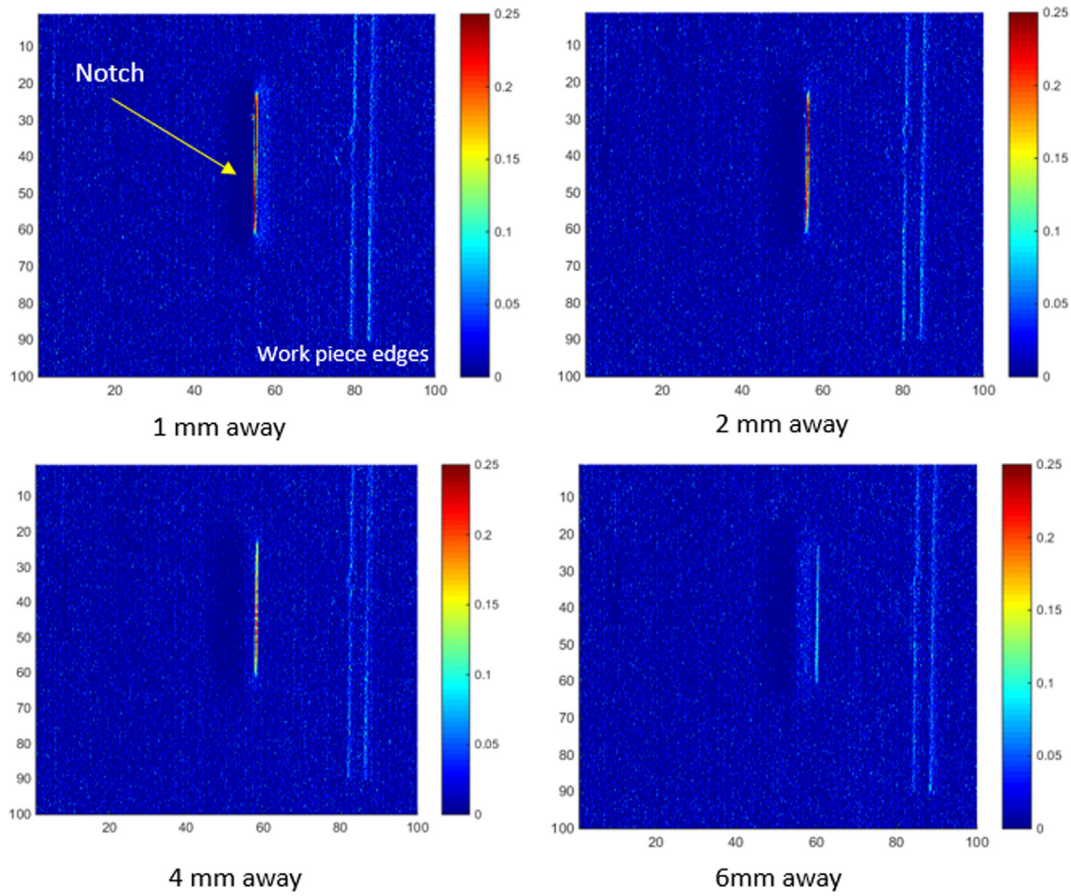

Fig. 16. Processed image: Laser Line is 1 mm, 2 mm, 4 mm and 6 mm away from the notch.

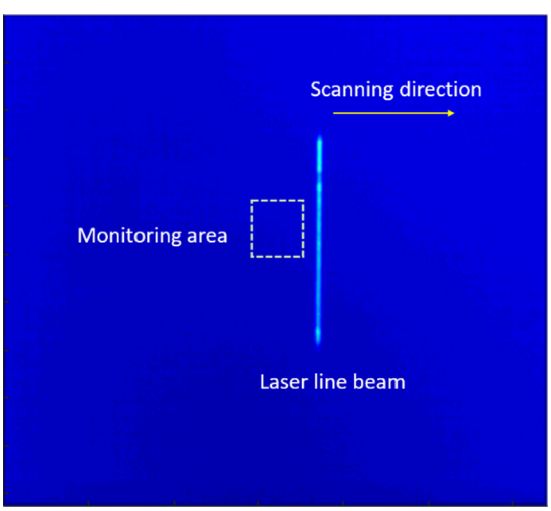

Fig. 17. Schematic of Laser scanning.

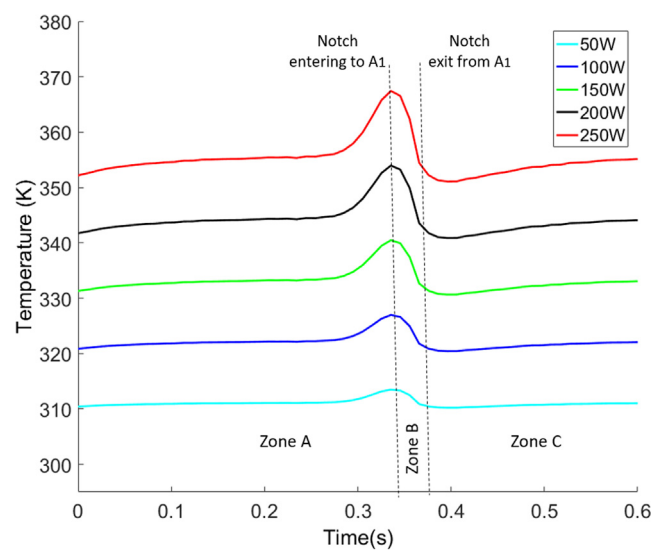

Fig. 18. Average temperature of the area A_1 using FEM simulation.

(TTRL) in numerical modeling, and the effect of TTRL in heat conduction was compared with an experimental defect. Both the experimental and modeling results gave the same trends and comparable results. The validated model can be used for future parameter studies to optimize the parameters which affect defect detectability and to improve the process parameter through improved feedback system.

Declaration of Competing Interest

Author declares that there is no conflicts of interest.

Acknowledgments

This work is financially supported by Indo-German Science and Technological Centre (IGSTC) under the project entitled Advanced Manufacturing Process Monitoring using in-line LASer Thermography (AMPLAST).

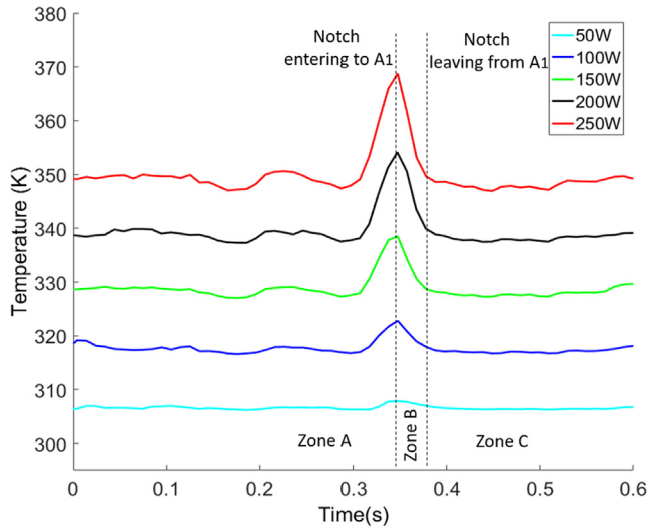

Fig. 19. Average temperature of the area A_1 from experiment.

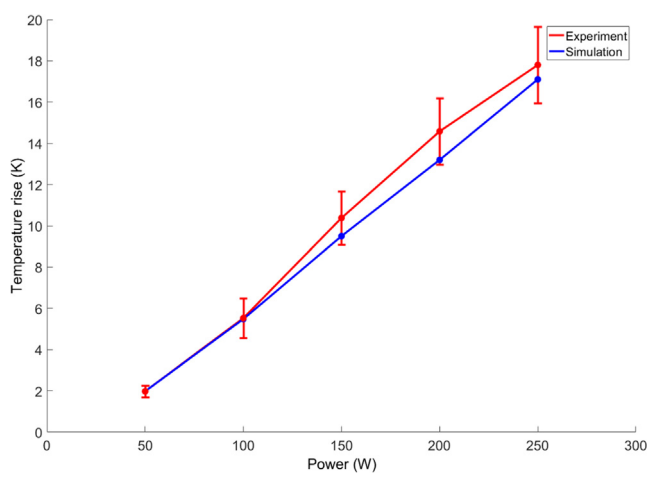

Fig. 20. Peak temperature rise Vs input laser power for line source : A comparison between FEM and experimental result.

References

[1] J. R. Davis, ASM Handbook: Nondestructive evaluation and quality control, vol. 17. ASM International, 1989.

[2] G.C. Holst, Testing and evaluation of infrared imaging systems, JCD Pub. (1998).

[3] X. Maldague, S. Marinetti, Pulse phase infrared thermography, J. Appl. Phys. 79 (5) (1996) 2694–2698.

[4] N. Puthiyaveettil, S. Krishna, R. Kidangan, S. Unnikrishnakurup, C.V. Krishnamurthy, In-line laser thermography for crack detection at elevated temperature : a numerical modeling study, QIRT2016 Proc. (2016) 588–596.

[5] J. Schlichting, M. Ziegler, A. Dey, C. Maierhofer, M. Kreutzbruck, Efficient data evaluation for thermographic crack detection, Quant. Infrared Thermogr. J. 8 (1) (2011) 119–123.

[6] X. Maldague, F. Galmiche, A. Ziadi, Advances in pulsed phase thermography, Infrared Phys. Technol. 43 (3–5) (2002) 175–181.

[7] E.J. Kubiak, Infrared detection of fatigue cracks and other near-surface defects, Appl. Opt. 7 (9) (1968) 1743–1747.

[8] R. Yang, Y. He, Optically and non-optically excited thermography for composites: A review, Infrared Phys. Technol. 75 (2016) 26–50.

[9] Y.K. An, J. Min Kim, H. Sohn, Laser lock-in thermography for detection of surface-breaking fatigue cracks on uncoated steel structures, NDT E Int. 65 (2014) 54–63.

[10] P. Broberg, Surface crack detection in welds using thermography, NDT E Int. 57 (2013) 69–73.

[11] S.E. Burrows, A. Rashed, D.P. Almond, S. Dixon, Combined laser spot imaging thermography and ultrasonic measurements for crack detection, Nondestruct. Test. Eval. 22 (2–3) (2007) 217–227.

[12] T. Li, D.P. Almond, D.A.S. Rees, Crack imaging by scanning laser line thermography, AIP Conf. Proc. 1335 (1) (2011) 407–414.

[13] S. Hwang, Y.-K. An, H. Sohn, Continuous-wave line laser thermography for monitoring of rotating wind turbine blades, Struct. Health Monitor. 147592171877170 (2018), https://doi.org/10.1177/1475921718771709.

[14] D. Jiao, Z. Liu, W. Zhu, W. Shi, H. Xie, Linear laser fast scanning thermography Ndt for artificial disbond defects in thermal barrier coatings, Optic Exp. 25 (2017) 2–3.

[15] D. Jiao, W. Shi, Z. Liu, H. Xie, Laser multi-mode scanning thermography method for fast inspection of micro-cracks in TBCs surface, J. Nondestruct. Eval. 37 (2) (2018) 1–10.

[16] S.E. Burrows, S. Dixon, S.G. Pickering, T. Li, D.P. Almond, Thermographic detection of surface breaking defects using a scanning laser source, NDT E Int. 44 (7) (2011) 589–596.

[17] Z.B. Hou, R. Komanduri, General solutions for stationary/moving plane heat source problems in manufacturing and tribology, Int. J. Heat Mass Transf. 43 (10) (2000) 1679–1698.

[18] V.P. Vavilov, Modeling thermal NDT problems, Int. J. Heat Mass Transf. 72 (2014) 75–86.

[19] C. Bu, Q. Tang, Y. Liu, X. Jin, Z. Sun, Z. Yan, A theoretical study on vertical finite cracks detection using pulsed laser spot thermography (PLST), Infrared Phys. Technol. 71 (2015) 475–480.

[20] J. Schlichting, C. Maierhofer, M. Kreutzbruck, Crack sizing by laser excited thermography, NDT E Int. 45 (1) (2012) 133–140.

[21] N.W. Pech-May, A. Oleaga, A. Mendioroz, A. Salazar, Fast characterization of the width of vertical cracks using pulsed laser spot infrared thermography, J. Nondestruct. Eval. 35 (2) (2016) 1–10.

[22] J. Qiu, C. Pei, H. Liu, Z. Chen, Quantitative evaluation of surface crack depth with laser spot thermography, Int. J. Fatigue 101 (2017) 80–85.